SHOCK AND REGOLITH FEATURES IN NORTHWEST AFRICA 15199. L. Louwerse[1,2], P. J. A. McCausland[1,2], and R. L. Flemming[1,2], [1]Institute for Earth & Space Exploration, University of Western Ontario, London, Ontario N6A 3K7, Canada. [2]Department of Earth Sciences, University of Western Ontario, London, Ontario N6A 5B7, Canada. llouwers@uwo.ca

Introduction: The Howardite-Eucrite-Diogenite (HED) clan of achondrite meteorites is likely derived from material that originated on the asteroid 4 Vesta[1,2]. Diogenites are orthopyroxene-rich rocks thought to have formed deep within the crust of 4 Vesta[2,3], whereas the basaltic eucrites are thought to have formed nearer to the surface[2]. Billions of years of impacts on the surface of 4 Vesta have resulted in the mixing of diogenites and eucrites to form the regolith breccias known as howardites[2,3]. Some impacts have excavated material from 4 Vesta, possibly generating the V-type asteroids[4] and the HED meteorites[1,2]. Thus, each HED provides valuable insights into the history of 4 Vesta, an asteroid from which samples have not yet been returned. We have recently classified the meteorite Northwest Africa (NWA) 15199 (Meteoritical Bulletin 111, forthcoming), found in Morocco and purchased by a private collector in 2021. Herein we classify NWA 15199 as a howardite and estimate the instantaneous shock pressure experienced by the meteorite and the temperature recorded by pyroxene geothermometers.

Samples and Methods: The 895.8 g meteorite NWA 15199 was cut to produce a 25.04 g type-specimen slab, an epoxy mounted offcut, and an approximately 2.9 cm^2 polished thin section. Magnetic susceptibility measurements were obtained from the slab using a Sapphire Instruments SI2b susceptibility meter. Bulk density measurements were obtained using the Archimedean method. Grain density measurements were made using a Quantachrome Multipycnometer with He gas. The polished thin section was used for all further analyses. Optical microscopy was conducted using a Nikon Eclipse LV100POL polarized light microscope. Micro X-Ray Diffraction (μXRD) analysis[5] was conducted using a Bruker D8 Discover micro X-ray diffractometer equipped with a Cobalt-K_α X-ray source, a 60 mm Gobel mirror, and a 300 μm pinhole collimator. Measurements were made in omega-scan mode with two 2-D General Area Detector Diffraction System (GADDS) frames collected per target. Frames were processed using DIFFRAC.EVA software to produce integrated intensity vs. 2θ plots which were then compared to International Centre for Diffraction Data diffraction patterns. For targets identified as plagioclase, plots of intensity vs. χ were produced for Full Width Half Maximum (FWHMχ) determination to estimate shock pressures. X-ray fluorescence (XRF) element maps were obtained using a Bruker M4 Tornado micro XRF instrument. Backscattered electron (BSE) imaging, silicon drift energy dispersive spectrometry (EDS), and quantitative chemical analyses were conducted using a JEOL JXA-8530F Field Emission Electron Probe Microanalyzer (EPMA).

Results and Discussion: *Physical Characteristics and Optical Analysis.* Cut faces of the stone show it to be a grey, feldspathic breccia of dark groundmass and lighter colour, angular igneous clasts, suggestive of an HED achondrite. The type specimen was found to have a magnetic susceptibility of $\log\chi(\times10^{-9}\ m^3/kg)=2.88$, consistent with howardites[6]. It has a bulk density of $3.17\pm0.01\ g/cm^3$, close to the average bulk density values for brecciated HEDs[7], and a grain density of $3.106\pm0.005\ g/cm^3$, yielding an effective porosity of zero. Optical analysis of the thin section revealed the meteorite to be composed of angular to sub-rounded brecciated lithic and crystalline clasts, up to 2.5 mm in the longest dimension. Under reflected light, several highly reflective grains between 0.1 mm and 3 mm in diameter were identified as oxides and sulphides. Under cross-polarized light (XPL), grains exhibited undulatory to mosaic extinction, indicating moderate shock, and a shock stage of S3 was assigned. Under plane polarized light (PPL) and XPL terrestrial weathering products were found filling cracks throughout the thin section, and a weathering grade of W3 was assigned.

μXRD Analysis. On the polished section, 32 targets were selected for μXRD analysis: 14 matched to ferroan enstatite, 4 to pigeonite, and 5 to anorthite. Other targets contained chromite, hematite, and veins containing troilite were identified. Pervasive calcite, a terrestrial weathering product, was also found. All anorthite targets exhibited streaking in the χ direction in their GADDS images. From these streaks, FWHMχ values were obtained and compared to an experimentally determined plagioclase reference curve[8], which yielded shock pressures ranging from approximately 13 GPa to 24 GPa. These pressures are consistent with our petrographic assignment of shock stage S3 and with the range of shock pressures reported in HEDs[9,10].

XRF. Qualitative element maps of the thin section were produced using XRF for common and anticipated elements. Fe, Ti, and Mg maps revealed that the sample contained two distinct lithologies (Fig. 1a), supporting visual and μXRD observations. Ca and K maps revealed plagioclase and calcite in the sample (Fig. 1b), and together with Fe and Mn maps revealed the grain size differences in the two lithologies. The dominant lithology made up approximately 88% of the thin section, and the volumetric makeup of the meteorite is observed to be similar. The Cr map revealed chromite grains and discontinuous curvilinear formations of chromium within pyroxene grains in the dominant lithology. S maps lend support to the presence of sulphide in veins of fine-grained material.

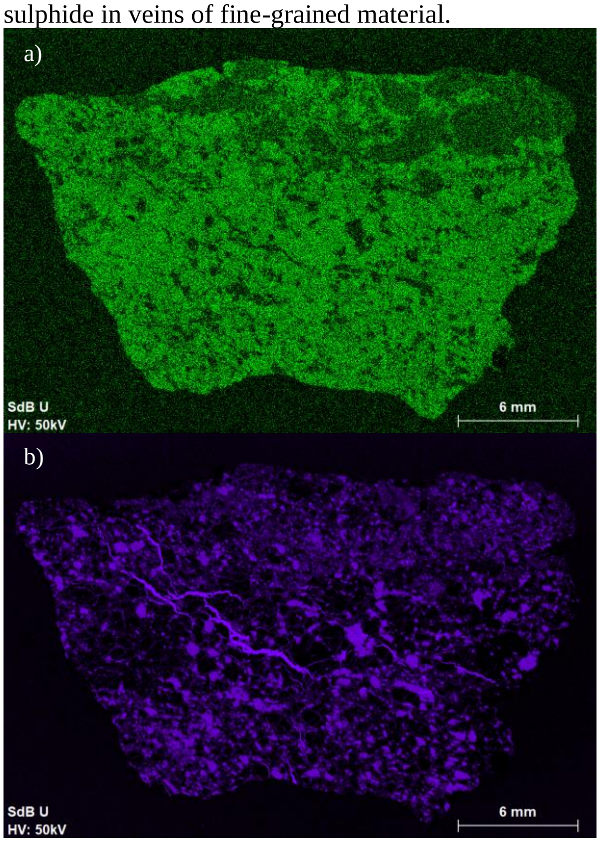

Fig. 1. XRF maps of the thin section depicting a) magnesium and b) calcium, which together highlight the two observed lithologies in the thin section.

BSE imaging and EDS. For each of the 32 targets chosen for µXRD, BSE images were captured to assist with target selection for EPMA chemical analysis. These images revealed that the pyroxene grains in the subordinate lithology exhibited exsolution lamellae. In addition, the fine-grained veins were shown to be flecked with sulphides, supporting the identification of troilite in these veins. The curvilinear features in chromite were confirmed to be associated with pyroxene grains. In addition, calcite and a sulphate were found to be present near or within most of the 32 targets. Using EDS, this sulphate was determined to be the terrestrial weathering product barite[11].

EPMA Analysis. For each of the 32 targets, typically 3 to 6 spots were selected for elemental analysis. In cases where the targets were more complex, as many as 9 spots were chosen. Pyroxene targets in the dominant lithology had compositions of $Fs_{33.7\pm1.0}Wo_{2.6\pm0.6}$ with Fe/Mn=28.0 (n=43). This affirmed the dominant lithology as diogenitic, with the Fe/Mn ratio matching that of HEDs[12]. Pyroxene targets in the subordinate lithology had compositions of $Fs_{56.5\pm2.2}Wo_{5.1\pm2.8}$ with Fe/Mn=31.9 (n=11) with the compositions of their exsolution lamellae being $Fs_{26.7\pm2.1}Wo_{41.4\pm0.6}$ with Fe/Mn=31.7 (n=8). This indicated that the subordinate lithology was eucritic, which established the meteorite as a howardite. Compositions for pigeonite and augite lamellae were used as a pyroxene geothermometer[13,14] to estimate a formation temperature of approximately 800°C. Plagioclase in the dominant lithology is anorthitic, $An_{93.2\pm0.8}$ (n=20), whereas plagioclase in the eucritic lithology is bytownite, $An_{85.6\pm1.6}$ (n=10).

Conclusions: The meteorite NWA 15199 was classified as a howardite, containing two mechanically distinct lithologies, one diogenitic and one eucritic. Micro-XRD analysis of plagioclase grains yielded peak shock pressures ranging from 13 GPa to 24 GPa. Crack-filling chromite in pyroxene grains in the diogenite lithology may have been mobilized during a shock event[15], and are notably absent from the eucritic lithology. The fine-grained troilite-bearing material that runs in veins between grains appears to be the product of another process, perhaps vapor deposition of sulphides in the breccia, and is less closely related to the diogenitic lithology.

Acknowledgments: We thank G. Abdelfattah and S. de Boer for providing sample of this meteorite to establish type specimen and enable this study. LL acknowledges WGRS M.Sc. funding support. PJAM and RLF acknowledge continuing support from NSERC Discovery grants.

References: [1] Binzel R.P. & Xu S. (1993) *Science*, *260*, 5105, 186–191. [2] McSween H.Y. Jr. et al. (2010) *Space Sci. Rev.*, *163*, 141–174. [3] Mandler B.E. & Elkins-Tanton L.T. (2013) *Meteorit. Planet. Sci.*, 48, 11, 2333–2349. [4] Fulvio D. et al. (2018) *Planet. Space Sci.*, *164*, 1, 37–43. [5] Flemming R. (2007) *Can. J. Earth Sci.*, *44*, 9, 1333–1346. [6] Rochette P. et al. (2009) *Meteorit. Planet. Sci.*, *44*, Nr. 3, 405–427. [7] Britt D.T. & Consolmagno G.J. (2003) *Meteorit. Planet. Sci.*, *38*, Nr. 8, 1161–1180. [8] Cao, F. et al. (2022) *IMA 2022*, Abstract #1578. [9] Takeda H. (1986) *P. Lunar Planet. Sci. XVI, Pt. 2, J. Geophys. Res.*, *91*, Nr. B4, D355–D363. [10] Pang R.–L. et al. (2016) *Sci. Rep.-UK*, *6*, Article #26063. [11] Lee M.R. & Bland P.A. (2004) *Geochim. Cosmochim. Ac.*, *68*, 4, 893–916. [12] Papike J.J. et al. (2003) *Am. Mineral.*, *88* (2–3), 469–472. [13] Lindsley D.H. (1983) *Am. Mineral.*, *68*, 477–493. [14] Lindsley D.H. & Anderson D.J. (1983) *P. Lunar Planet. Sci. XIII, Pt. 2, J. Geophys. Res.*, *88*, Supplement, A997–A906. [15] Rubin A.E. & Ma C. (2017) *Chem. Erde-Geochem.*, *77*, 325–385.